

FINITE STRAIN MODEL FOR ELASTOMER–ALUMINIUM CONTACT INTERFACE IN FORMING PROCESSES

Mariela Luege , Bibiana M. Luccioni

Instituto de Estructuras, Universidad Nacional de Tucumán, CONICET
Av. Roca 1800, S.M. de Tucumán, 4000 Tucumán, Argentina
e-mail: mluege@herrera.unt.edu.ar

Key words: Friction law, lubrication, computational contact, forming processes

Summary. *In this paper we introduce a phenomenological friction law for the continuous sliding of a polymer on a surface of aluminum for lubricated and dry conditions as it occurs in metal forming processes. The contact model is developed within the framework of continuum thermodynamics of irreversible processes with internal variables and for large strains assuming the contact area as a material surface. The model is able to describe the boundary friction map proposed in [1].*

1 INTRODUCTION

The frictional behaviour of a surface sliding with respect to another, separated by a lubricant fluid of viscosity η_b , and with contact area A is usually described by a single curve called the Stribeck curve (see Figure 1(a)). This curve assumes $AV\eta_b/D$ as the relevant parameter in defining the friction force F . As a result, decreasing the film thickness D by one-half has the same effect as doubling the sliding velocity V . However, such behaviour is not verified in experiments. On the basis of experimental findings, [1] propose the more reliable friction map of Figure 1(b). The friction force is defined as function of V and is represented in terms of a family of curves parameterized by D or the applied normal load L . Distinguishing features of these curves are the existence of three regimes: bulk, intermediate and pure frictional. The bulk regime ($D = 250\text{--}180\text{ nm}$) is characterized by a viscous response and a constant viscosity equal to the viscosity of the lubricant. In the pure frictional regime a Coulomb like behaviour is noted, whereas in the intermediate one both the aspects are present with the existence of a value of the sliding velocity V depending on D (or on L) that signs the transition to the viscous regime (see Figure 1(b)).

Aim of this note is to develop a thermodynamically consistent model that reproduces the above experimentally observed behaviour and apply it to model the elastomer–aluminium interface.

2 KINEMATIC AND THERMODYNAMICAL FRAMEWORK

For the kinematic representation of the contact we follow the notation and definition of [4, 5]. Let \mathcal{B}^i , $i = 1, 2$, denote the two bodies that come in contact, $\Omega^i \in \mathbb{R}^3$, $i = 1, 2$, the respective reference configuration, and Γ_c^i the part of $\partial\Omega^i$ that at the time t are in

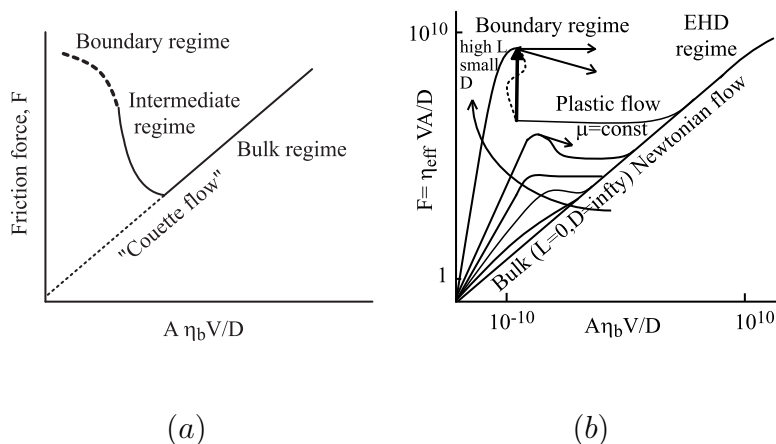


Figure 1: (a) Stribeck curve in the case of lubrication. (b) Boundary friction map

contact, the contact conditions are parameterized by $\mathbf{X} \in \Gamma_c^1$ by means of the closest projection point $\bar{\mathbf{Y}}(\mathbf{X}, t) = \arg \min_{\mathbf{Y} \in \Gamma_c^2} |\varphi_t^i(\mathbf{X}) - \varphi_t^i(\mathbf{Y})|$ with φ_t^i deformation of \mathcal{B}^i at time t . Furthermore, with each point \mathbf{X} we associate a slip advected bases (\mathbf{T}_α) defined on the sliding surface Γ_c^2 [4, 5]. Given the slip distance $\mathbf{g}_T(\mathbf{X}) = \int_{t_s}^t \xi^{\dot{\alpha}} \mathbf{T}_\alpha d\tau$, with $\xi^{\dot{\alpha}}$ components of the tangential relative velocity between \mathbf{X} and $\bar{\mathbf{Y}}(\mathbf{X}, t)$, t_s the time when contact starts occurring and t the current time, we consider the additive decomposition $\mathbf{g}_T = \mathbf{g}_T^e + \mathbf{g}_T^p$, with \mathbf{g}_T^e related to the elastic micro deformations part of the asperities, and \mathbf{g}_T^p to the permanent surface slip. Considering the contact area Γ_c as a material boundary [2, 3], the Clausius–Duhem inequality reads as

$$\mathcal{D} = t_N \dot{g} + \mathcal{T}_T \cdot \mathcal{L}_V \mathbf{g}_T - \dot{\psi} \geq 0, \quad (1)$$

with ψ the surface free energy, t_N and \mathcal{T}_T the normal and tangential component of the contact force, respectively, \dot{g} the time derivative of the gap function, and $\mathcal{L}_V \mathbf{g}_T$ the Lie derivative of \mathbf{g}_T with respect to the velocity $\mathbf{V}^{(2)}$ [4, 5]. A thermodynamically consistent model is obtained by giving the free energy ψ and evolution laws so that (1) is met.

3 THE CONTACT MODEL

Given the frictional behaviour of Figure 1(b), for $D \leq D_{min}$ we consider a Coulomb type behaviour with friction coefficient $\mu = \mu_d + \frac{\mu_s - \mu_d}{1 + \langle d_{\mathbf{g}_T^p} - A_d \rangle_+ B}$, where μ_s and μ_d denote the static and kinetic value, respectively, $d_{\mathbf{g}_T^p} = \int_{t_0}^t |\mathcal{L}_V \mathbf{g}_T^p| dt$ the accumulated sliding distance, B an interface material parameter, and A_d a characteristic slip distance. For $D \geq D_{max}$ the contact law is of a Newtonian fluid with viscosity η_b , whereas for $D_{min} \leq D \leq D_{max}$ on Γ_c the surface free energy is chosen as

$$\psi(g, \mathbf{g}_T, \mathbf{g}_T^p) = \frac{1}{2} K_N g^2 + I_{x \geq 0}(g) + (1 - \alpha) \frac{1}{2} K_T |\mathbf{g}_T - \mathbf{g}_T^p|^2, \quad (2)$$

with $\alpha = \min \left\{ \left(\frac{\langle D - D_{min} \rangle_+}{D_{max} - D_{min}} \right)^\beta, 1 \right\}$ if $|\mathcal{L}_V \mathbf{g}_T|$ is lower than the limit value $\sqrt{\frac{\gamma D_{max}}{\eta_b D}}$, otherwise α is set equal to one. The constant γ is a parameter that must be fitted to the experimental results of Figure 1(b) further to some assumptions on the curves in the transition regime, whereas β is a parameter depending on the current thickness. In (2) $I_{x \geq 0}$ is the indicator function of \mathbb{R}_+ introduced to describe the impenetrability condition, whereas K_N and K_T are parameters as in [3].

The state laws relating the state variables $(g, \mathbf{g}_T, \mathbf{g}_T^p)$ to the dual thermodynamic forces $(t_N^e, \mathcal{T}_T^e, \mathcal{W}^p)$ are obtained from (1) as follows

$$t_N^e - K_N g \in \partial I_{x \geq 0}(g) \Leftrightarrow g \geq 0, \quad (t_N^e - K_N g)g = 0, \quad t_N^e - K_N g \leq 0$$

$$\mathcal{T}_T^e = \frac{\partial \psi}{\partial \mathbf{g}_T} = (1 - \alpha) K_T \mathbf{g}_T^e, \quad \mathcal{W}^p = -\frac{\partial \psi}{\partial \mathbf{g}_T^p} = \mathcal{T}_T^e. \quad (3)$$

We introduce the dissipation potential

$$\Phi(\mathcal{L}_V \mathbf{g}_T, \mathcal{L}_V \mathbf{g}_T^p) = \mu |t_N^e| |\mathcal{L}_V \mathbf{g}_T^p| + \alpha \frac{\eta_b}{2} |\mathcal{L}_V \mathbf{g}_T|^2$$

with μ defined as above. The evolution laws are then given as $(t_N^i, \mathcal{T}_T^i, \mathcal{W}^p) \in \partial_{\mathbf{z}} \Phi(\mathbf{z}; \chi)$, that is,

$$t_N^i = 0, \quad \mathcal{T}_T^i = \alpha \eta_b \mathcal{L}_V \mathbf{g}_T, \quad \mathcal{L}_V \mathbf{g}_T^p = \lambda \frac{\mathcal{W}^p}{|\mathcal{W}^p|},$$

$$\mathcal{F} \leq 0, \quad \lambda \mathcal{F} = 0, \quad \lambda \geq 0. \quad (4)$$

with $\mathcal{F} := |\mathcal{W}^p| - \mu t_N^e \leq 0$ and use of duality has been invoked. From (4), it follows that the normal tension is elastic.

4 NUMERICAL EXAMPLE

The proposed model is compared in this section with the experimental results of [1] obtained using the Surface Forces Apparatus. After the two surfaces are brought into contact, the upper surface is moved laterally and applies a normal pressure of $3.0E6 \text{ N/m}^2$ kept constant during the process. Three different film thickness ($D = 10, 30, 180 \text{ nm}$) have been considered in the numerical simulation. The finite element model is described in Figure 2(a). For the numerical integration of the contact law, we use the backward Euler and a predictor/corrector algorithm to solve the resulting nonlinear algebraic system. The integration scheme is performed using the slip advected basis that ensures frame invariance [4]. The model has been implemented in the dynamic explicit finite element code STAMPAK with the penalty formulation to handle the unilateral contact.

The constants used to define the constitutive model are: $D_{max} = 250 \text{ nm}$, $D_{min} = 0 \text{ nm}$, $\gamma = 4.0 E - 25$ and $\eta_b = 0.8 \text{ N s/m}^2$. For $D = 10 \text{ nm}$ and low velocities, the behaviour is almost of Coulomb type with $\alpha = 0.039$ and $\beta = 1.0$. For $D = 30 \text{ nm}$ and $D = 180 \text{ nm}$ the

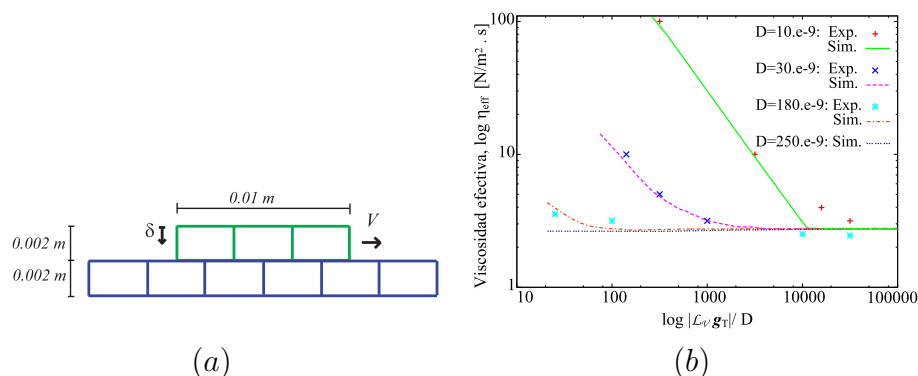


Figure 2: (a) Finite element model with plane strain quadrilateral elements using 4 Gauss points. (b) Effective viscosity vs. Sliding velocity.

interface parameters are $\alpha = 0.9967$, $\beta = 0.01$ and $\alpha = 0.9999$, $\beta = 0.00001$, respectively. For these values of D the influence of the frictional behaviour decreases with respect to the viscous one, even though the effective viscosity $\eta_{eff} = FD/(VA)$ is greater than η_b . Also, for values of the velocity greater than $\sqrt{\frac{\gamma D_{max}}{\eta_b D}}$ one recovers the viscous Newton type behaviour. The latter is clearly also exhibited for $D = D_{max}$.

REFERENCES

- [1] G. Luengo, F.-J. Schmitt, R. Hill and J. Israelachvili. Thin film rheology and tribology of confined polymer melts: Contrasts with bulk properties. *Macromolecules*, **30**, 2482–2494, 1997.
- [2] N. Stroemberg, L. Johansson and A Klarbring. Derivation and analysis of a generalized standard model for contact, friction and wear. *In. J. Solids Structures*, **33**, 1817–1836, 1996.
- [3] M. Raous, L. Cangémi and M. Cocu. A consistent model coupling adhesion, friction and unilateral contact. *Comput. Methods Appl. Mech. Engrg.*, **177** 383–399, 1999.
- [4] T.A. Laursen. *Computational Contact and Impact Mechanics*, Springer, 2002.
- [5] P. Wriggers *Computational Contact Mechanics*, Jhn Wiley & Sons, 2002